

Rotation-Symmetric Bosonic Code Error Correction

Investigating error-correcting capabilities of the Two-Mode Binomial Code

Project report: TRA200, Building and Programming a Quantum Computer

Julius Andersson, Griffin Hiscoke, Carl Svensson, Hang Zou

Abstract

This project investigates the error-correcting capabilities of the Two-Mode Binomial Code, a subclass of Rotation-Symmetric Bosonic (RSB) codes designed to mitigate the trade-off between protection against photon loss and dephasing noise. The project focuses exclusively on the ability of the code to correct photon loss errors. While the Knill-Laflamme (KL) conditions for this code are known to be satisfied to the first order in the photon decay rate, its behavior at higher orders has not been previously established. We derive the two-mode photon loss error operators to the second order in κt and evaluate the satisfaction of the KL conditions for code parameters $K = 2$ with symmetry orders $N = 2$ and $N = 4$. By utilizing a cost function to quantify the violation of these conditions, our results demonstrate that the KL conditions are not strictly satisfied for either symmetry order. However, the $N = 4$ code shows a higher degree of satisfaction compared to $N = 2$, with optimal beam-splitter parameters found at $\delta = \pi/4$ and $3\pi/4$. This corresponds to the values required for first-order dephasing correction. These findings indicate that while exact error correction is not feasible to the second order, the $N = 4$ Two-Mode Binomial Code remains a promising candidate for use with approximate recovery channels such as teleportation or the Petz Recovery Map.

Contents

1	Introduction	1
1.1	Aim & Goal	1
2	Background	2
2.1	Rotation-Symmetric Bosonic (RSB) Codes	2
2.1.1	Error Detecting Properties	3
2.1.2	Binomial Code	4
2.2	Quantum Error Correction	5
2.2.1	Kraus Representation	5
2.2.2	Knill-Laflamme Conditions	6
3	Methods	7
3.1	Expanding the Two-Mode Photon Loss Operators to Second Order	7
3.2	Checking KL-conditions	7
4	Results	9
5	Conclusion	12
5.1	Outlook	12
A	Appendix	13
A.1	Derivation of Second Order Operators	13
A.2	All Error Operator Combinations	15
A.3	Derivation of Annihilation Operator Transformation	16

1 Introduction

Quantum computers are expected to solve certain problems more efficiently than classical computers. Notably, quantum algorithms for integer factorization [1] and unstructured search [2] have been proven to be asymptotically faster than the best-known classical algorithms. Additionally, a demonstration of *quantum advantage* was reported for a 53-qubit quantum processor, which performed a task estimated to take 10,000 years for a classical computer [3]. Another area in which quantum computers are expected to outperform classical systems is the simulation of quantum mechanics [4].

Active research is currently underway in the field of quantum computing, primarily following two approaches: Discrete-Variable (DV) and Continuous-Variable (CV). In the DV approach, finite-dimensional Hilbert spaces are used to encode information. Prominent examples include the Transmon [5] and Fluxonium [6] qubits, both of which are based on superconducting circuits. A harmonic oscillator is typically used to perform the readout of the quantum state [7].

In contrast, CV systems utilize the infinite-dimensional Hilbert space of a harmonic oscillator to encode information [8] using bosonic modes. The name “continuous-variable” arises from the fact that the quantum state is described by continuous degrees of freedom, such as field quadratures, rather than by discrete variables like energy levels in DV systems. Although CV systems do not form physical qubits (two-level systems) naturally, it is possible to engineer states that function as two-level systems. These are referred to as logical qubits and can be realized using bosonic codes.

Due to the infinite-dimensional Hilbert space available in CV quantum computing, a wide variety of bosonic codes can be constructed. Two major classes are the Gottesman-Kitaev-Preskill (GKP) codes [9] and Rotationally Symmetric Bosonic (RSB) codes [10]. RSB codes offer protection against photon loss and dephasing, two of the most dominant error channels in bosonic systems. However, a trade-off exists: increasing protection against one type of error typically reduces robustness against the other.

The Two-Mode Binomial Code, a specific type of RSB code proposed by researchers at Chalmers [11], overcomes this specific trade-off and therefore shows promise for error correction. The Knill-Laflamme (KL) conditions, which determine whether errors can be corrected exactly, have been shown to be satisfied to the first order in the photon decay rate for this code. This confirms the possibility of exact recovery from these errors up to the first order. However, the performance at higher orders remains unknown. By studying the KL conditions for higher orders, the capabilities of the Two-Mode Binomial code as a candidate for quantum error correction can be better understood.

1.1 Aim & Goal

Given this, the aim of the project is to:

1. Verify the Knill-Laflamme conditions to second order in κt for photon-loss for the Two-Mode Binomial Code for
 - (a) $N=2, K=2$
 - (b) $N=4, K=2$
2. Conditioned on KL-conditions being satisfied in 1, derive the recovery channel to second order in κt .

2 Background

Two prominent classes of bosonic codes are the GKP Codes [9] and the RSB Codes [10]. GKP codes utilize translational symmetry, while RSB codes instead utilize rotational symmetry. Our work is about the Two-Mode Binomial Code [11], belonging to the RSB class.

2.1 Rotation-Symmetric Bosonic (RSB) Codes

Rotation-Symmetric Bosonic Codes are a class of codes characterized by discrete rotational symmetry. Specifically, they are defined as the $+1$ eigenstates of the discrete rotation operator $R_N = e^{i(2\pi/N)\hat{n}}$, where N is the order of symmetry. We denote the logical states $|0\rangle$ and $|1\rangle$ for an order- N code as $|0_N\rangle$ and $|1_N\rangle$, respectively.

While the operator R_N acts as the identity operator on the order- N RSB code, $R_{2N} = e^{i(2\pi/2N)\hat{n}} = e^{i(\pi/N)\hat{n}}$ acts as the logical Z operator (\bar{Z}) and is therefore referred to as Z_N . These properties are summarized by the following relations:

$$R_N |\mu_N\rangle = e^{i(2\pi/N)\hat{n}} |\mu_N\rangle = + |\mu_N\rangle, \quad (1a)$$

$$Z_N |\mu_N\rangle = e^{i(\pi/N)\hat{n}} |\mu_N\rangle = (-1)^\mu |\mu_N\rangle, \quad (1b)$$

where $\mu \in \{0, 1\}$.

The order- N RSB code can be viewed both in terms of its rotation, and photon number spacing. It can be constructed by superposing a primitive code $|\Theta\rangle$ with different discrete rotations as

$$|0_N\rangle = \frac{1}{\sqrt{\mathcal{N}_0}} \sum_{m=0}^{2N-1} e^{i(\pi m/N)\hat{n}} |\Theta\rangle, \quad (2a)$$

$$|1_N\rangle = \frac{1}{\sqrt{\mathcal{N}_1}} \sum_{m=0}^{2N-1} (-1)^m e^{i(\pi m/N)\hat{n}} |\Theta\rangle, \quad (2b)$$

where $\mathcal{N}_{0/1}$ are normalization constants and N the order of symmetry. The choice of primitive $|\Theta\rangle$ and symmetry order N enable wide customization of RSB codes. By choosing different primitive codes, one can construct, among others, the Cat, Squeezed, and Binomial codes [10]. An equivalent way of writing the same order- N RSB code is as a superposition of Fock-states as

$$|0_N\rangle = \sum_{k=0}^{\infty} f_{2kN} |2kN\rangle, \quad (3a)$$

$$|1_N\rangle = \sum_{k=0}^{\infty} f_{(2k+1)N} |(2k+1)N\rangle, \quad (3b)$$

where f_{kN} are coefficients. Any superposition of them will therefore consist solely of Fock states with number N -spacing. These properties are visualized in Fig. 1

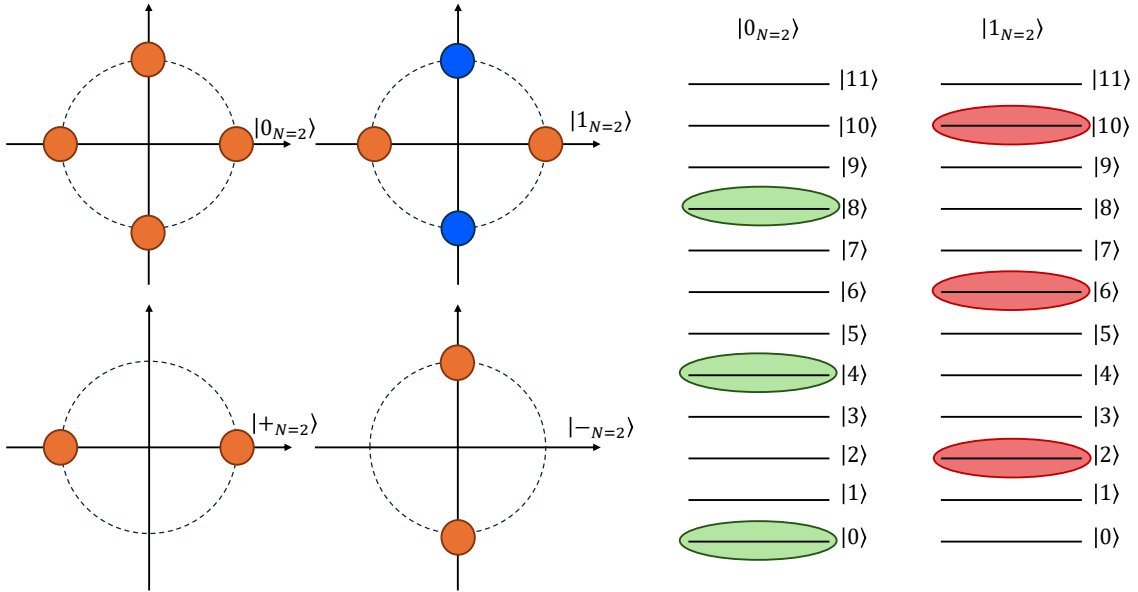


Figure 1: Illustration of RSB-code rotational symmetry (left) and Fock-state spacing (right). Left: Phase space representation for an $N = 2$ RSB code constructed from coherent states $|\pm\alpha\rangle$, showing logical basis states and superposition states. Orange indicates positive values, and blue indicates negative values. Right: Fock space representation of the order- $N = 2$ bosonic code. Inspired by similar figures in Ref. [10]

2.1.1 Error Detecting Properties

The ability to describe the RSB code in terms of rotational symmetry and Fock-state spacing provides a powerful framework for quantum error correction. Two of the most prominent physical errors types for bosonic codes are photon loss and dephasing. The occurrence of photon loss can be detected by performing a photon number measurement. If no photon loss has occurred, the measurement gives a photon number $n \bmod N = 0$, since $|0_N\rangle$ ($|1_N\rangle$) are even (odd) multiples of N . Thus, measuring $n \bmod N \neq 0$ signals the occurrence of photon loss. Assuming the absence of photon gain, the RSB-code can correct up to $N - 1$ -photon loss events, since the loss of N photons would constitute a bit-flip. We therefore say that the RSB code has code distance $d_n = N$ for photon loss. Likewise, we can distinguish the superposition states $|+_N\rangle$ and $|-_N\rangle$ by performing a phase measurement of θ in $e^{i\theta\hat{n}}|\Theta\rangle$. If no dephasing has occurred, the measurement gives $\theta \bmod \pi/N = 0$, as is easily seen from Eq. (2). Thus, if $\theta \bmod \pi/N \neq 0$, then dephasing has occurred. The code distance for dephasing noise is $d_\theta = \pi/N$.

The expressions for the code distances show a trade-off between the robustness against photon loss errors and dephasing errors for RSB codes. Increasing the symmetry order (N), makes the spacing between the rotated primitives smaller, while at the same time making the photon number spacing larger. This decreases the number of dephasing errors that are correctable while increasing the ones for photon loss errors. This can be illustrated by looking at $|+_N\rangle$ and $|0_N\rangle$ for $N = 2$ and $N = 4$. This is shown in Fig. 2

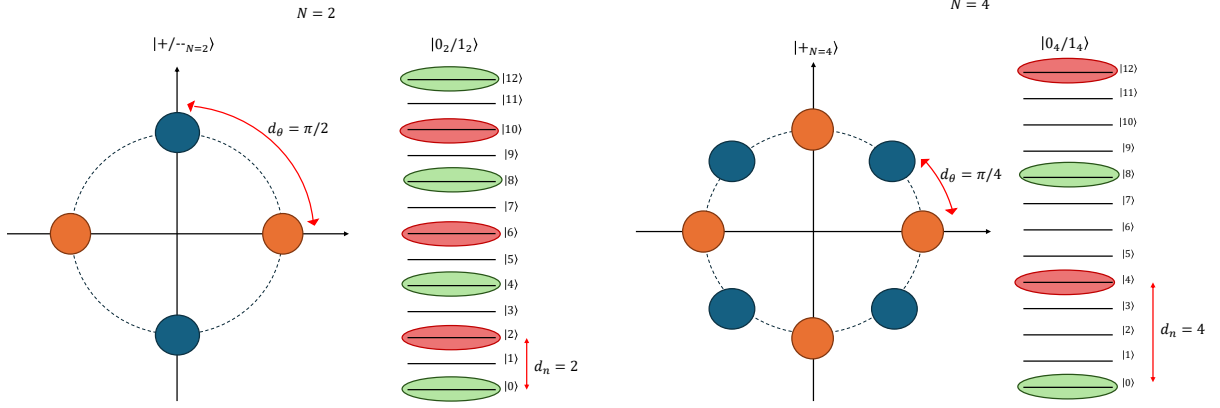


Figure 2: Illustration showing the impact of the symmetry order N on the dephasing (left) and photon loss error (right) detection. The left figures show for $N = 2$ and the right figures show for $N = 4$. Orange is $|+N\rangle$, navy-blue $|-N\rangle$, green $|0_N\rangle$, and red $|1_N\rangle$. Inspired by similar figures in Ref. [10]

2.1.2 Binomial Code

The Binomial code, which the Two-Mode-Binomial Code is based on, was first introduced in 2016 [12], and has the form

$$|0_{N,\text{bin}}\rangle = \sum_{k=0}^{\lfloor K/2 \rfloor} \sqrt{\frac{1}{2^{K-1}} \binom{K}{2k}} |2kN\rangle, \quad (4a)$$

$$|1_{N,\text{bin}}\rangle = \sum_{k=0}^{\lfloor K/2 \rfloor - 1} \sqrt{\frac{1}{2^{K-1}} \binom{K}{2k+1}} |(2k+1)N\rangle, \quad (4b)$$

where $|0_{N,\text{bin}}\rangle$ and $|1_{N,\text{bin}}\rangle$ are the logical qubits, $\lfloor x \rfloor$ the floor function, and K an integer determining the truncation of the Fock-states. The name "binomial" refers to the fact that the coefficients are given by the square root of binomially distributed weights. Taking $K = 2$, we get the binomial codes

$$|0_N\rangle = \frac{1}{\sqrt{2}} (|0\rangle + |2N\rangle), \quad |1_N\rangle = |N\rangle \quad (5)$$

Two-Mode RSB codes are constructed as tensor products of the corresponding single-mode codes. In particular, the two-mode logical $|0\rangle$ is formed as the tensor product of the single-mode logical $|0\rangle$ and $|1\rangle$, whereas the two-mode logical $|1\rangle$ is given by the tensor product $|1\rangle$ and $|0\rangle$. Note the ordering of the modes. This ensures that the two-mode logical qubit base states are orthogonal. A general expression for a Two-Mode RSB code is

$$|0_N\rangle = \hat{U}_{\text{BS}}(\delta, \phi) \sum_{m,n} f_{mn} |2mN\rangle \otimes |(2n+1)N\rangle, \quad (6a)$$

$$|1_N\rangle = \hat{U}_{\text{BS}}(\delta, \phi) \sum_{m,n} f_{mn} |(2n+1)N\rangle \otimes |2mN\rangle, \quad (6b)$$

where $\hat{U}_{BS}(\delta, \phi)$ is a beam-splitter, n and m positive integer numbers, and f_{mn} the coefficients. The beam-splitter has the expression

$$\hat{U}_{BS}(\delta, \phi) = \exp[\delta(a_2^\dagger a_1 e^{i\phi} - a_1^\dagger a_2 e^{-i\phi})], \quad (7)$$

where a_1 and a_1^\dagger (a_2 and a_2^\dagger) are the bosonic operators acting on the first (second) mode. It, thus, entangles the two modes.

The Two-Mode Binomial code [11] has shown to eliminate the trade-off between robustness against photon loss and dephasing noise, and therefore shows great promise. The Two-Mode Binomial $K = 2$ code can be formed from Eq. (5) by inputting it into Eq. (6). It then gets the form

$$|0_N\rangle = U_{BS}(\delta, \phi) \frac{1}{\sqrt{2}}(|0\rangle + |2N\rangle) \otimes |N\rangle, \quad (8a)$$

$$|1_N\rangle = U_{BS}(\delta, \phi) |N\rangle \otimes \frac{1}{\sqrt{2}}(|0\rangle + |2N\rangle). \quad (8b)$$

2.2 Quantum Error Correction

As previously discussed, quantum codes are susceptible to various noise channels. The dominant physical error source is photon loss [13], though dephasing also plays a significant role. Photon gain is theoretically possible but is typically suppressed at cryogenic temperatures.

These physical error mechanisms can result in leakage from the code space, as well as logical errors (\bar{X} , \bar{Y} , \bar{Z}) within the code space. While a code does not prevent the physical errors from occurring, a well designed one mitigates the effects of them.

The performance of RSB codes varies depending on the specific error channel. As noted earlier, robustness against photon loss and dephasing relies heavily on the symmetry order N , as well as the choice of code primitives. For instance, the $N = 1$ cat code has been shown to be robust against photon loss, even in the absence of a recovery map [14]. In contrast, the same does not hold for the $K = 2$ binomial code, as its constituent Fock states are eventually annihilated after successive applications of the lowering operator.

To model the impact of noise on the quantum state evolution, several approaches are available, including the Kraus representation [15], the Master equation [16], and Quantum Trajectories [17]. In this work, we employ the Kraus representation.

2.2.1 Kraus Representation

The Kraus Representation models the evolution of the density matrix. The density matrix ($\hat{\rho}$) is formed by taking the sum of all possible state vectors

$$\hat{\rho} = \sum_i |\psi_i\rangle \langle \psi_i|, \quad (9)$$

where $|\psi_i\rangle$ is a state vector. In the Kraus-representation, the state at time t is determined by

$$\hat{\rho}(t) = \sum_l \hat{K}_l(t) \hat{\rho}(0) \hat{K}_l^\dagger(t), \quad (10)$$

where $\hat{\rho}(0)$ and $\hat{\rho}(t)$ are the initial and final state, and $K_l(t)$ the Kraus operator. The Kraus operators have the property

$$\sum_l \hat{K}_l^\dagger(t) \hat{K}_l(t) = I, \quad (11)$$

where I is the identity matrix.

Photon loss is represented by the Kraus operators

$$\hat{L}_l(t) = \sqrt{\frac{[1 - e^{-\kappa t}]^l}{l!}} e^{-\frac{\kappa t}{2} \hat{a}^\dagger \hat{a}} \hat{a}^l. \quad (12)$$

where l corresponds to a loss of l photons and κ is the photon decay rate. Other types of errors have different Kraus operators. For instance, the Kraus operator for dephasing is

$$D_l = \sqrt{\frac{\gamma t}{l!}} e^{-\frac{\gamma t}{2} (\hat{a}^\dagger \hat{a})^2} (\hat{a}^\dagger \hat{a})^l, \quad (13)$$

where γ is the dephasing rate.

In the two-mode case, we write the density matrix as the tensor product of the single mode density matrices as

$$\hat{\rho}_{12} = \hat{\rho}_1 \otimes \hat{\rho}_2, \quad (14)$$

where $\hat{\rho}_{12}$ is the two-mode density matrix, and $\hat{\rho}_1$ ($\hat{\rho}_2$) the density matrix for the first (second) mode. The resulting photon loss Kraus operators similarly become tensor products of the single mode ones. The resulting Kraus operators become

$$\hat{L}_{lm} = \hat{L}_l \otimes \hat{L}_m = \sqrt{\frac{[1 - e^{-\kappa_1 t}]^l}{l!}} e^{-\frac{\kappa_1 t}{2} \hat{a}_1^\dagger \hat{a}_1} \hat{a}_1^l \otimes \sqrt{\frac{[1 - e^{-\kappa_2 t}]^m}{m!}} e^{-\frac{\kappa_2 t}{2} \hat{a}_2^\dagger \hat{a}_2} \hat{a}_2^m, \quad (15)$$

where l (m) is the number of photons lost in the first (second) mode.

2.2.2 Knill-Laflamme Conditions

The errors inflicted on the system limits the performance of the quantum codes and are ideally avoided. In case errors do occur, a recovery map can be implemented to correct for the errors. Important for recovery maps is the Knill-Laflamme condition, which states that if

$$\langle i | E_\alpha E_\beta | j \rangle = \delta_{ij} C_{\alpha\beta}, \quad (16)$$

then a recovery map exists such that the errors can be perfectly corrected. Here E_α and E_β are Kraus operators for a specific error, belonging to $\{E\}$, $i, j \in 0, 1$, δ_{ij} is the Kronecker delta function, and $C_{\alpha\beta}$ is a constant depending solely on the errors and not the states.

The two-mode binomial code in Eq. (8) satisfied the KL-condition to first order in Eq. (15) for $N = 2$ and $N = 4$. While it does not satisfy the KL-conditions for two-mode dephasing for $N = 2$, it does so for $N = 4$, but only for the beam-splitter parameters $\delta = \pi/4, 3\pi/4$.

In case the KL-condition is not satisfied, it is still possible to quantify how well it is or is not satisfied. In previous work [18, 19, 20], the following cost function has been used

$$C_{\text{KL}}(\hat{E}) = \sum_{a,b} |f_{00ab} - f_{11ab}|^2 + |f_{01ab}|^2, \quad (17)$$

where $f_{ijab} = \langle i | \hat{E}_a^\dagger \hat{E}_b | j \rangle$. The term $|f_{00ab} - f_{11ab}|^2$ quantifies the state dependence of the coefficient $C_{\alpha\beta}$ for the two different states, and $|f_{01ab}|^2$ the magnitude of the off-diagonal terms. Only f_{01ab} is considered as it already captures the same information as f_{10ab} .

Even if the KL-conditions are not satisfied, it is still possible to create an approximate recovery map. Two prominent approaches for bosonic codes are using teleportation [21], which can correct leakage errors, and the Petz recovery map [22].

3 Methods

3.1 Expanding the Two-Mode Photon Loss Operators to Second Order

The first step of the project consisted of approximating the error operators $\{\hat{L}_{lm}\}$ to second order in $\kappa_i t, i = 1, 2$. It should be noted that the requirement of being at most second order applies to the error induced by the operator, not the operator itself. An operator may be second order in form, yet produce exclusively higher order errors. Those operators are therefore not viewed as second order and henceforth ignored.

We first approximated the single-mode photon loss operators to second order. Due to the the very small timescales involved, any higher order terms quickly become tiny. We observed that the only operators appearing at second order were $\hat{L}_0, \hat{L}_1,$ and \hat{L}_2 . \hat{L}_3 was technically below second order ($\hat{L}_3 \propto (\kappa t)^{3/2}$), but the error it would cause would be of higher order ($\hat{L}_3 \hat{L}_3^\dagger \propto (\kappa t)^3$), and it was therefore not included. The two-mode operators were thereafter derived from the combinations of these three, yielding nine possible combinations. Of these nine, only six were at most second order: $\hat{L}_{21}, \hat{L}_{12},$ and \hat{L}_{22} gave exclusively higher order errors. Thus, only a total loss of two photons in the modes was possible at second order. A more in depth derivation is given in Appendix A.1.

3.2 Checking KL-conditions

In order to check the KL-conditions, we had to derive the possible error combinations $E_\alpha^\dagger E_\beta$, where $E_\alpha, E_\beta \in \{L_{lm}\}$. Several remarks are in order regarding this calculation.

First, it is not necessary to derive hermitian conjugates. This is preferable, because the error combinations yield many terms. Instead, one can observe that the KL-conditions for the hermitian conjugate of $E_\alpha^\dagger E_\beta$ and $E_\beta^\dagger E_\alpha$, are checked for $\langle i_N | E_\beta^\dagger E_\alpha | j_N \rangle = (\langle j_N | E_\alpha^\dagger E_\beta | i_N \rangle)^*$, where we have taken the hermitian conjugate. This simplifies the derivation significantly. By taking this into account, we get a total of 21 error combinations, which are approximated to second order. These combinations are shown in Appendix A.2.

Second, the presence of the beam-splitter $\hat{U}_{BS}(\delta, \phi)$ presents difficulties in the calculations. Applying it to the Fock-states, as is done in Eq. (8), involves a Taylor expansion of the beam-splitter and is ideally avoided. A more efficient approach is to apply the beam-splitter to the error combinations instead.

This is done by dividing the Two-mode binomial code in Eq. (8) into two parts: the beam-splitter $\hat{U}_{BS}(\delta, \phi)$ and the Fock-states: We define

$$|\tilde{0}_N\rangle = \frac{1}{\sqrt{2}}(|0\rangle + |2N\rangle) \otimes |N\rangle, \quad |\tilde{1}_N\rangle = |N\rangle \otimes \frac{1}{\sqrt{2}}(|0\rangle + |2N\rangle), \quad (18)$$

and then obtain the logical qubits by applying the beam-splitter,

$$|0_N\rangle = \hat{U}_{BS}(\delta, \phi) |\tilde{0}_N\rangle, \quad |1_N\rangle = \hat{U}_{BS}(\delta, \phi) |\tilde{1}_N\rangle. \quad (19)$$

Inputting Eq. (19) into the KL-conditions in Eq. (16), we get the following expression

$$\langle i_N | E_\alpha^\dagger E_\beta | j_N \rangle = \langle \tilde{i}_N | \underline{U_{BS}^\dagger(\delta, \phi) E_\alpha^\dagger E_\beta U_{BS}(\delta, \phi)} | \tilde{j}_N \rangle. \quad (20)$$

The underlined term constitutes an operator transformation, and we can therefore work with Eq. (18) instead of Eq. (8) when we check the KL-conditions. The beam-splitter is a unitary operator, meaning that $\hat{U}_{BS}(\delta, \phi) \hat{U}_{BS}^\dagger(\delta, \phi) = \hat{U}_{BS}^\dagger(\delta, \phi) \hat{U}_{BS}(\delta, \phi) = I$, where I is the identity operator. This relation can therefore be inserted multiple times into the error combinations, simplifying the calculations even further: Every bosonic operator in the error combinations just has to be transformed as $b_i = \hat{U}_{BS}^\dagger(\delta, \phi) a_i \hat{U}_{BS}(\delta, \phi)$,

$i = 1, 2$. The transformation is given in Ref [11] as

$$\hat{a}_1 \rightarrow \hat{b}_1 = \hat{U}_{\text{BS}}^\dagger(\delta, \phi) \hat{a}_1 \hat{U}_{\text{BS}}(\delta, \phi) = \hat{a}_1 \cos \delta + \hat{a}_2 e^{-i\phi} \sin \delta, \quad (21a)$$

$$\hat{a}_2 \rightarrow \hat{b}_2 = \hat{U}_{\text{BS}}^\dagger(\delta, \phi) \hat{a}_2 \hat{U}_{\text{BS}}(\delta, \phi) = \hat{a}_2 \cos \delta - \hat{a}_1 e^{+i\phi} \sin \delta, \quad (21b)$$

but we additionally show the derivation in Appendix A.3.

It is not feasible to verify the KL-conditions by hand for these transformed error combinations, as they give rise to lengthy and highly complex expressions. We therefore wrote a Mathematica script to do the remaining analytical calculations. The calculated matrix elements f_{ijab} were shown in Mathematica. Our Mathematica script, as well as the rest of the code we used for plotting the results, is given in Ref. [23].

4 Results

Our calculations show that the KL-conditions are not satisfied for either $N = 2$ or $N = 4$, neither in general nor for any specific values for the beam-splitter parameters (δ, ϕ) . The transformations in Eq. (21) gave terms with dependence on δ and ϕ . Specifically, the terms contained expressions with sinusoidal dependence on δ , as well as complex phase factors dependent on ϕ . From our script, we immediately saw that the KL-conditions were not satisfied for $N = 2$, since multiple off-diagonal terms, $\langle i | E_\alpha^\dagger E_\beta | j \rangle$ ($i \neq j$), were non-zero. It was not possible to make the terms vanish by any choice of beam-splitter parameters or the decay rates $\kappa_i t$ $i = 1, 2$. This was because some terms needed $\cos \delta = 0$, while others needed $\sin \delta = 0$; satisfying both conditions simultaneously is impossible. The diagonal terms ($i = j$) were also not independent of the state for $N = 2$, which is also a required condition. The KL-conditions first appeared to be satisfied for $N = 4$, since all the off-diagonal elements were zero. The diagonal terms for $N = 4$ were, however, not independent of the state, but only dependent on δ and not ϕ . All terms were dependent on both δ and ϕ for $N = 2$.

The degree to which the KL-conditions were close to being satisfied was investigated by plotting the cost function (17) for $N = 2$ and $N = 4$. The result is shown in Fig. 3. For $N = 4$, it was immediately obvious that the best satisfaction was given for $\delta = \pi/4, 3\pi/4$. This corresponded to the values for which the KL-conditions for the dephasing channel were satisfied to first order. Setting different values of $\kappa_1 t$ and $\kappa_2 t$ did not change this. The same was not true for $N = 2$. There, the minimums depended on the values of the decay rates in the two modes. For $\kappa_1 t = \kappa_2 t = 10^{-2}$, the minimums occurred for values of $\phi = 0, \pi$ as well as values slightly perturbed from $\delta = \pi/4, 3\pi/4$. For $\kappa_1 t = 10^{-2}$ and $\kappa_2 t = 10^{-3}$ the optimal values of ϕ were instead close to $\phi = \pi/4, 3\pi/4$, for the same values of δ .

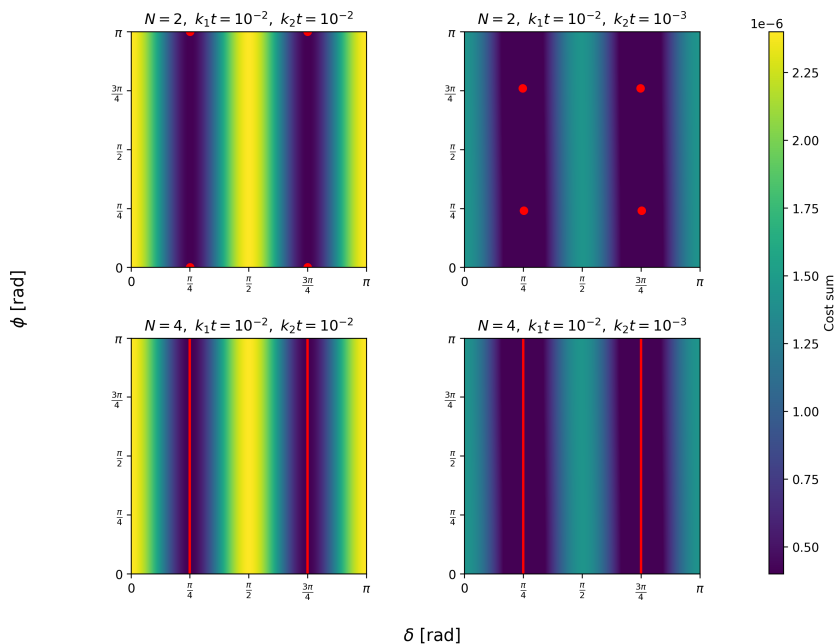


Figure 3: Heatmap of the cost function for $N = 2$ (upper) and $N = 4$ (lower) for $\kappa_1 t = 10^{-2}$ and $\kappa_2 t = 10^{-2}$ (left), and $\kappa_1 t = 10^{-2}$ and $\kappa_2 t = 10^{-3}$ (right). The beam-splitter parameters (δ, ϕ) giving the lowest value for the cost function are highlighted in red. Vertical lines are shown for $N = 4$, since there was no dependence on ϕ .

One can observe that greater values of the cost function were obtained for $N = 4$ than $N = 2$. We do not think that this has any importance for the satisfaction of the KL-conditions. The reason why higher values are observed is because the Two-Binomial code with $N = 4$ consists of higher Fock-states. Applying the bosonic operators yields greater values, which then results in a higher valued cost function. Similarly, lower values of the cost function are observed for $\kappa_1 t = 10^{-2}$, $\kappa_2 t = 10^{-3}$ for both $N = 2$ and $N = 4$. This is logical, since the matrix elements were proportional to powers of $\kappa_i t$, $i = 1, 2$. A lower value of $\kappa_2 t$ should therefore lead to lower values of the cost function. At the same time, the physical meaning of having a lower decay rate is that there are fewer losses which in practice would result in fewer violations of the KL conditions. This is however a property of all bosonic codes, so it does not give any information about the relative performance of this specific code.

In order to get information about the contribution of the different error combinations $E_\alpha^\dagger E_\beta$, we also plot these for the optimal beam-splitter parameters (δ, ϕ) , in Fig. 4. As can be seen, most error combinations exactly satisfy the KL-conditions, but several still do not. For $N = 2$, certain combinations vanish or remain non-zero for different values of the decay rates. For $\kappa_1 t = \kappa_2 t = 10^{-2}$, $E_1^\dagger E_1$, $E_2^\dagger E_2$, and $E_3^\dagger E_3$ vanish, while they are non-zero for $\kappa_1 t = 10^{-2}$ and $\kappa_2 t = 10^{-3}$. This is because the contributing matrix elements were proportional to $(\kappa_1 t - \kappa_2 t)$. Although the same dependence was present for $N = 4$, new error combination contributions do not occur for a change in decay rates. This is because the terms depending on the difference in the decay rates were also proportional to sinusoidal terms depending on δ , which vanish for $\delta = \pi/4, 3\pi/4$.

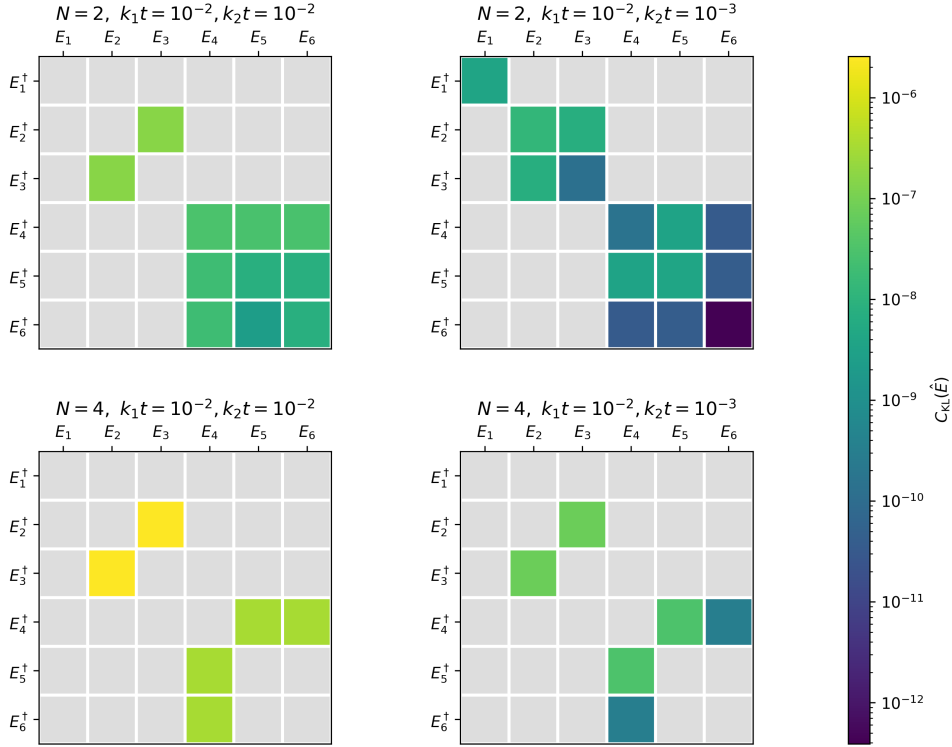


Figure 4: Logarithmic plot of the contribution of all the error combinations to the cost function for $N = 2$ (upper) and $N = 4$ (lower) for $\kappa_1 t = 10^{-2}$ and $\kappa_2 t = 10^{-2}$ (left), and $\kappa_1 t = 10^{-2}$ and $\kappa_2 t = 10^{-3}$ (right). Grey is 0 meaning the condition is satisfied.

Possible errors in our calculations include analytical ones, done by hand, and errors done by incorrect Mathematica scripts. The presence or absence of errors in our calculations can be verified by reading through our code, found on GitHub [\[23\]](#), or reading through our analytical calculations.

5 Conclusion

In this work, we evaluated the Knill-Laflamme (KL) conditions for the Two-Mode Binomial code (truncated to $K = 2$) specifically against second-order photon loss errors for symmetry orders $N = 2$ and $N = 4$. Our analysis reveals that the conditions for this second-order error channel are not strictly satisfied for either $N = 2$ or $N = 4$, regardless of the specific beam-splitter parameters (δ, ϕ) . Although the conditions are never fully met, we observed that the degree of violation is lower for $N = 4$ compared to $N = 2$. Notably, the optimal beam-splitter parameters identified here align with those reported in previous studies for the first-order dephasing channel, suggesting a consistent optimal regime for this code. However, the precise quantitative relationship between the degree of KL-condition satisfaction and the achievable error-correction fidelity remains an open question.

5.1 Outlook

Future investigations could extend this evaluation to higher symmetry orders ($N > 4$). This extension is straightforward, as the computational framework (Mathematica script) developed herein can be readily adapted. Furthermore, the KL conditions should be evaluated for second-order dephasing errors. To facilitate this, the computational tools should be unified and automated, enabling efficient exploration of the code parameter space. Finally, future work should attempt to construct an approximate recovery channel for second-order photon loss, potentially utilizing techniques such as teleportation-based recovery or the Petz recovery map [24].

A Appendix

A.1 Derivation of Second Order Operators

The starting point is the single-mode photon loss Kraus operator

$$\hat{L}_l(t) = \sqrt{\frac{[1 - e^{-\kappa t}]^l}{l!}} e^{-\frac{\kappa t}{2} \hat{a}^\dagger \hat{a}} \hat{a}^l.$$

Everything except the \hat{a}^l should be Taylor expanded. It is, however, not possible to Taylor expand the whole expression, since $\sqrt{\frac{[1 - e^{-\kappa t}]^l}{l!}}$ has a non-existing derivative at $\kappa t = 0$ for $l > 0$. Instead, one has the Taylor expand to individual terms to second order.

It is trivial to see that to second order

$$\hat{L}_0 \approx 1 - \frac{\kappa t}{2} \hat{a}^\dagger \hat{a} + \frac{(\kappa t)^2}{8} (\hat{a}^\dagger \hat{a})^2,$$

since $\sqrt{\frac{[1 - e^{-\kappa t}]^0}{0!}} = \hat{a}^0 = 0$, and only $e^{\frac{\kappa t}{2} \hat{a}^\dagger \hat{a}}$ can be Taylor expanded. For $l > 0$ it is however not as simple. Instead, we have to do some mathematical tricks.

Note that

$$\begin{aligned} \sqrt{[1 - e^{-\kappa t}]^l} &= [1 - e^{-\kappa t}]^{l/2} = \left\{ e^x = 1 + x + \frac{1}{2}x^2 + \dots \right\} = \left[1 - \left(1 - \kappa t + \frac{(\kappa t)^2}{2!} - \frac{(\kappa t)^3}{3!} + \dots \right) \right]^{l/2} \\ &= \left[\kappa t - \frac{(\kappa t)^2}{2!} + \frac{(\kappa t)^3}{3!} - \dots \right]^{l/2} = (\kappa t)^{l/2} \left[1 - \frac{(\kappa t)}{2!} + \frac{(\kappa t)^2}{3!} - \dots \right]^{l/2}. \end{aligned}$$

We then use the binomial formula with the value inside $[]^{l/2}$ as x

$$(1 + x)^{l/2} = \sum_{k=0}^{\infty} \binom{l/2}{k} x^k, \quad x = -\frac{\kappa t}{2!} + \frac{(\kappa t)^2}{3!} - \dots$$

and get

$$\begin{aligned} &\Rightarrow \left[1 - \frac{(\kappa t)}{2!} + \frac{(\kappa t)^2}{3!} - \dots \right]^{l/2} = \sum_{k=0}^{\infty} \binom{l/2}{k} \left[-\frac{\kappa t}{2!} + \frac{(\kappa t)^2}{3!} - \dots \right]^k \\ &\approx 1 + \frac{l}{2} \left[-\frac{\kappa t}{2!} + \frac{(\kappa t)^2}{3!} - \dots \right] + \frac{l}{2} \left(\frac{l}{2} - 1 \right) \left[-\frac{\kappa t}{2!} + \frac{(\kappa t)^2}{3!} - \dots \right]^2 \\ &\approx 1 - \frac{l}{4} \kappa t + \frac{l}{12} (\kappa t)^2 + \frac{l}{8} \left(\frac{l}{2} - 1 \right) (\kappa t)^2 \end{aligned}$$

We have to take into account the $(\kappa t)^{l/2}$ term that was factored out. Because of this, only the terms up to first order in κt from the binomial expansion survives. The same is true from the Taylor expansion of $e^{\frac{\kappa t}{2} \hat{a}^\dagger \hat{a}}$. Putting everything together, we get the following expression that can be used to determine the single mode photon loss operators (\hat{L}_l) to second order

$$\hat{L}_l \approx \frac{1}{\sqrt{l!}} (\kappa t)^{l/2} \left[1 - \frac{l}{4} \kappa t \right] \left[1 - \frac{\kappa t}{2} \hat{a}^\dagger \hat{a} \right] \hat{a}^l$$

We keep only terms that are at most second order:

$$\begin{aligned}
\hat{L}_1 &\approx (\kappa t)^{1/2} \left[1 - \frac{1}{4} \kappa t \right] \left[1 - \frac{\kappa t}{2} \hat{a}^\dagger \hat{a} \right] \hat{a} \approx (\kappa t)^{1/2} \left[1 - \frac{1}{4} \kappa t - \frac{1}{2} \kappa t \hat{a}^\dagger \hat{a} \right] \hat{a} \\
&= \left[(\kappa t)^{1/2} - \frac{1}{4} (\kappa t)^{3/2} - \frac{1}{2} (\kappa t)^{3/2} \hat{a}^\dagger \hat{a} \right] \hat{a} \\
\hat{L}_2 &\approx \frac{1}{\sqrt{2}!} \kappa t \left[1 - \frac{1}{2} \kappa t \right] \left[1 - \frac{\kappa t}{2} \hat{a}^\dagger \hat{a} \right] \hat{a}^2 \approx \frac{1}{\sqrt{2}!} \kappa t \left[1 - \frac{1}{2} \kappa t - \frac{1}{2} \kappa t \hat{a}^\dagger \hat{a} \right] \hat{a}^2 \\
&= \frac{1}{\sqrt{2}!} \left[\kappa t - \frac{1}{2} (\kappa t)^2 - \frac{1}{2} (\kappa t)^2 \hat{a}^\dagger \hat{a} \right] \hat{a}^2 \approx \frac{1}{\sqrt{2}!} (\kappa t) \hat{a}^2 \\
\hat{L}_3 &\approx \frac{1}{\sqrt{6}} (\kappa t)^{3/2} \left[1 - \frac{3}{4} \kappa t \right] \left[1 - \frac{\kappa t}{2} \hat{a}^\dagger \hat{a} \right] \hat{a}^3 \approx \frac{1}{\sqrt{6}} (\kappa t)^{3/2} \hat{a}^3 \quad (\hat{L}_3 \hat{\rho} \hat{L}_3^\dagger \propto (\kappa t)^3)
\end{aligned}$$

\hat{L}_x , where $x > 2$, will only give higher order effects, and can therefore be ignored. The results of our calculations are shown below:

$$\begin{aligned}
\hat{L}_0 &= 1 - \frac{\kappa t}{2} \hat{a}^\dagger \hat{a} + \frac{(\kappa t)^2}{8} (\hat{a}^\dagger \hat{a})^2 \\
\hat{L}_1 &= \left[(\kappa t)^{1/2} - \frac{1}{4} (\kappa t)^{3/2} - \frac{1}{2} (\kappa t)^{3/2} \hat{a}^\dagger \hat{a} \right] \hat{a} \\
\hat{L}_2 &= \frac{1}{\sqrt{2}} (\kappa t) \hat{a}^2
\end{aligned}$$

Our next task is to write all possible two-mode operators (\hat{L}_{lm}) to second order. Since we have 3 one-mode operators, we will have at most $3 \cdot 3 = 9$ two-mode operators. Some of these might only include higher order terms and therefore be approximated as zero. We write the two mode operators as \hat{E}_n :

$$\begin{aligned}
\hat{E}_1 = \hat{L}_{00} &= \hat{L}_0^1 \hat{L}_0^2 \approx 1 - \frac{\kappa_1 t}{2} \hat{a}_1^\dagger \hat{a}_1 - \frac{\kappa_2 t}{2} \hat{a}_2^\dagger \hat{a}_2 + \frac{(\kappa_1 t)(\kappa_2 t)}{4} (\hat{a}_1^\dagger \hat{a}_1)(\hat{a}_2^\dagger \hat{a}_2) + \frac{(\kappa_1 t)^2}{8} (\hat{a}_1^\dagger \hat{a}_1)^2 + \frac{(\kappa_2 t)^2}{8} (\hat{a}_2^\dagger \hat{a}_2)^2 \\
\hat{E}_2 = \hat{L}_{10} &= \hat{L}_1^1 \hat{L}_0^2 \approx (\kappa_1 t)^{1/2} \hat{a}_1 - \frac{(\kappa_1 t)^{1/2} (\kappa_2 t)}{2} \hat{a}_1 (\hat{a}_2^\dagger \hat{a}_2) - \frac{(\kappa_1 t)^{3/2}}{4} \hat{a}_1 - \frac{(\kappa_1 t)^{3/2}}{2} \hat{a}_1^\dagger \hat{a}_1 \hat{a}_1 \\
\hat{E}_3 = \hat{L}_{01} &= \hat{L}_0^1 \hat{L}_1^2 \approx (\kappa_2 t)^{1/2} \hat{a}_2 - \frac{(\kappa_2 t)^{1/2} (\kappa_1 t)}{2} (\hat{a}_1^\dagger \hat{a}_1) \hat{a}_2 - \frac{(\kappa_2 t)^{3/2}}{4} \hat{a}_2 - \frac{(\kappa_2 t)^{3/2}}{2} \hat{a}_2^\dagger \hat{a}_2 \hat{a}_2 \\
\hat{E}_4 = \hat{L}_{11} &= \hat{L}_1^1 \hat{L}_1^2 \approx (\kappa_1 t)^{1/2} (\kappa_2 t)^{1/2} \hat{a}_1 \hat{a}_2 \\
\hat{E}_5 = \hat{L}_{20} &= \hat{L}_2^1 \hat{L}_0^2 \approx \frac{1}{\sqrt{2}} (\kappa_1 t) (\hat{a}_1)^2 \\
\hat{E}_6 = \hat{L}_{02} &= \hat{L}_0^1 \hat{L}_2^2 \approx \frac{1}{\sqrt{2}} (\kappa_2 t) (\hat{a}_2)^2
\end{aligned}$$

$\hat{E}_7 - \hat{E}_9$ only give higher order effects on the error channel

A.2 All Error Operator Combinations

By using the six different two-mode photon loss operators derived in Appendix. A.1, the following error combinations are obtained to second order. Hermitian conjugates are not shown.

$$\begin{aligned}
\hat{E}_1^\dagger \hat{E}_1 &\approx 1 - (\kappa_1 t)(\hat{a}_1^\dagger \hat{a}_1) - (\kappa_2 t)(\hat{a}_2^\dagger \hat{a}_2) + (\kappa_1 t)(\kappa_2 t)(\hat{a}_1^\dagger \hat{a}_1)(\hat{a}_2^\dagger \hat{a}_2) + \frac{1}{2}(\kappa_1 t)^2(\hat{a}_1^\dagger \hat{a}_1)^2 + \frac{1}{2}(\kappa_2 t)^2(\hat{a}_2^\dagger \hat{a}_2)^2 \\
\hat{E}_1^\dagger \hat{E}_2 &\approx (\kappa_1 t)^{1/2} \hat{a}_1 - \frac{1}{4}(\kappa_1 t)^{3/2} \hat{a}_1 - (\kappa_1 t)^{3/2}(\hat{a}_1^\dagger \hat{a}_1) \hat{a}_1 - (\kappa_1 t)^{1/2}(\kappa_2 t) \hat{a}_1 (\hat{a}_2^\dagger \hat{a}_2) \\
\hat{E}_1^\dagger \hat{E}_3 &\approx (\kappa_2 t)^{1/2} \hat{a}_2 - (\kappa_1 t)(\kappa_2 t)^{1/2}(\hat{a}_1^\dagger \hat{a}_1) \hat{a}_2 - \frac{1}{4}(\kappa_2 t)^{3/2} \hat{a}_2 - (\kappa_2 t)^{3/2}(\hat{a}_2^\dagger \hat{a}_2) \hat{a}_2 \\
\hat{E}_1^\dagger \hat{E}_4 &\approx (\kappa_1 t)^{1/2}(\kappa_2 t)^{1/2} \hat{a}_1 \hat{a}_2 - \frac{1}{2}(\kappa_1 t)^{3/2}(\kappa_2 t)^{1/2}(\hat{a}_1^\dagger \hat{a}_1) \hat{a}_1 \hat{a}_2 - \frac{1}{2}(\kappa_1 t)^{1/2}(\kappa_2 t)^{3/2}(\hat{a}_2^\dagger \hat{a}_2) \hat{a}_2 \hat{a}_1 \\
\hat{E}_1^\dagger \hat{E}_5 &\approx \frac{1}{\sqrt{2}}(\kappa_1 t)(\hat{a}_1)^2 - \frac{1}{2\sqrt{2}}(\kappa_1 t)(\kappa_2 t)(\hat{a}_2^\dagger \hat{a}_2)(\hat{a}_1)^2 - \frac{1}{2\sqrt{2}}(\kappa_1 t)^2(\hat{a}_1^\dagger \hat{a}_1)(\hat{a}_1)^2 \\
\hat{E}_1^\dagger \hat{E}_6 &\approx \frac{1}{\sqrt{2}}(\kappa_2 t)(\hat{a}_2)^2 - \frac{1}{2\sqrt{2}}(\kappa_1 t)(\kappa_2 t)(\hat{a}_1^\dagger \hat{a}_1)(\hat{a}_2)^2 - \frac{1}{2\sqrt{2}}(\kappa_2 t)^2(\hat{a}_2^\dagger \hat{a}_2)(\hat{a}_2)^2 \\
\hat{E}_2^\dagger \hat{E}_2 &\approx (\kappa_1 t) \hat{a}_1^\dagger \hat{a}_1 - \frac{(\kappa_1 t)^2}{2} \hat{a}_1^\dagger \hat{a}_1 - (\kappa_1 t)^2(\hat{a}_1^\dagger)^2(\hat{a}_1)^2 - (\kappa_1 t)(\kappa_2 t)(\hat{a}_1^\dagger \hat{a}_1)(\hat{a}_2^\dagger \hat{a}_2) \\
\hat{E}_2^\dagger \hat{E}_3 &\approx (\kappa_1 t)^{1/2}(\kappa_2 t)^{1/2} \hat{a}_1^\dagger \hat{a}_2 - \frac{1}{4}(\kappa_1 t)^{1/2}(\kappa_2 t)^{3/2} \hat{a}_1^\dagger \hat{a}_2 - \frac{1}{4}(\kappa_1 t)^{3/2}(\kappa_2 t)^{1/2} \hat{a}_1^\dagger \hat{a}_2 - (\kappa_1 t)^{1/2}(\kappa_2 t)^{3/2}(\hat{a}_2^\dagger \hat{a}_2) \hat{a}_2 \hat{a}_1^\dagger \\
&\quad - (\kappa_1 t)^{3/2}(\kappa_2 t)^{1/2} \hat{a}_2 \hat{a}_1^\dagger (\hat{a}_1^\dagger \hat{a}_1) \\
\hat{E}_2^\dagger \hat{E}_4 &\approx (\kappa_1 t)(\kappa_2 t)^{1/2}(\hat{a}_1^\dagger \hat{a}_1) \hat{a}_2 \\
\hat{E}_2^\dagger \hat{E}_5 &\approx \frac{1}{\sqrt{2}}(\kappa_1 t)^{3/2} \hat{a}_1^\dagger (\hat{a}_1)^2 \\
\hat{E}_2^\dagger \hat{E}_6 &\approx \frac{1}{\sqrt{2}}(\kappa_1 t)^{1/2}(\kappa_2 t) \hat{a}_1^\dagger (\hat{a}_2)^2 \\
\hat{E}_3^\dagger \hat{E}_3 &\approx (\kappa_2 t) \hat{a}_2^\dagger \hat{a}_2 - \frac{1}{2}(\kappa_2 t)^2 \hat{a}_2^\dagger \hat{a}_2 - (\kappa_2 t)^2(\hat{a}_2^\dagger)^2(\hat{a}_2)^2 - (\kappa_1 t)(\kappa_2 t)(\hat{a}_1^\dagger \hat{a}_1) \hat{a}_2^\dagger \hat{a}_2 \\
\hat{E}_3^\dagger \hat{E}_4 &\approx (\kappa_1 t)^{1/2}(\kappa_2 t)^{3/2}(\hat{a}_2^\dagger \hat{a}_2) \hat{a}_1 \\
\hat{E}_3^\dagger \hat{E}_5 &\approx \frac{1}{\sqrt{2}}(\kappa_1 t)(\kappa_2 t)^{1/2} \hat{a}_2^\dagger (\hat{a}_1)^2 \\
\hat{E}_3^\dagger \hat{E}_6 &\approx \frac{1}{\sqrt{2}}(\kappa_2 t)^{3/2} \hat{a}_2^\dagger (\hat{a}_2)^2 \\
\hat{E}_4^\dagger \hat{E}_4 &\approx (\kappa_1 t)(\kappa_2 t) \hat{a}_1^\dagger \hat{a}_1 \hat{a}_2^\dagger \hat{a}_2 \\
\hat{E}_4^\dagger \hat{E}_5 &\approx \frac{1}{\sqrt{2}}(\kappa_1 t)^{3/2}(\kappa_2 t)^{1/2}(\hat{a}_1^\dagger \hat{a}_1) \hat{a}_1 \hat{a}_2^\dagger \\
\hat{E}_4^\dagger \hat{E}_6 &\approx \frac{1}{\sqrt{2}}(\kappa_1 t)^{1/2}(\kappa_2 t)^{3/2}(\hat{a}_2^\dagger \hat{a}_2) \hat{a}_2 \hat{a}_1^\dagger \\
\hat{E}_5^\dagger \hat{E}_5 &\approx \frac{1}{2}(\kappa_1 t)^2(\hat{a}_1^\dagger)^2(\hat{a}_1)^2 \\
\hat{E}_5^\dagger \hat{E}_6 &\approx \frac{1}{2}(\kappa_1 t)(\kappa_2 t)(\hat{a}_1^\dagger)^2(\hat{a}_2)^2 \\
\hat{E}_6^\dagger \hat{E}_6 &\approx \frac{1}{2}(\kappa_2 t)^2(\hat{a}_2^\dagger)^2(\hat{a}_2)^2
\end{aligned}$$

A.3 Derivation of Annihilation Operator Transformation

In order to understand the derivation, one first need to understand the meaning of commutation. The commutation between two operators \hat{A} and \hat{B} is defined as

$$[\hat{A}, \hat{B}] = \hat{A}\hat{B} - \hat{B}\hat{A}.$$

The commutator is important because the order in which operators are applied matters in quantum mechanics. The reason why this is not always zero can be understood by treating the operators as matrices. The resulting matrix is dependent on the order in which the matrices are applied, as is known from linear algebra. The commutation relation is widely used in quantum mechanics, see Ref. [25] for examples of its use. The annihilation and creation operators of the two modes have the commutation relations

$$\begin{aligned} [\hat{a}_i, \hat{a}_j^\dagger] &= \delta_{ij}, \\ [\hat{a}_i, \hat{a}_j] &= [\hat{a}_i^\dagger, \hat{a}_j^\dagger] = 0, \end{aligned}$$

where $i, j \in 1, 2$. When we have products of operators, the following rule can be applied:

$$[\hat{A}\hat{B}, \hat{C}\hat{D}] = \hat{A}[\hat{B}, \hat{C}\hat{D}] + [\hat{A}, \hat{C}\hat{D}]\hat{B} = \hat{A}\hat{C}[\hat{B}, \hat{D}] + \hat{A}[\hat{B}, \hat{C}]\hat{D} + \hat{C}[\hat{A}, \hat{D}]\hat{B} + [\hat{A}, \hat{C}]\hat{D}\hat{B},$$

where \hat{A} , \hat{B} , \hat{C} , and \hat{D} are all operators. The commutator is also linear

$$[\hat{A} + \hat{B}, \hat{C} + \hat{D}] = [\hat{A}, \hat{C} + \hat{D}] + [\hat{B}, \hat{C} + \hat{D}] = [\hat{A}, \hat{C}] + [\hat{A}, \hat{D}] + [\hat{B}, \hat{C}] + [\hat{B}, \hat{D}].$$

The commutation relations have great importance for the derivation of the transformed operators. This is through the Baker-Hausdorff Lemma, that states that

$$e^{\hat{A}}\hat{B}e^{-\hat{A}} = \hat{B} + [\hat{A}, \hat{B}] + \frac{1}{2!}[\hat{A}, [\hat{A}, \hat{B}]] + \frac{1}{3!}[\hat{A}, [\hat{A}, [\hat{A}, \hat{B}]]] + \frac{1}{4!}[\hat{A}, [\hat{A}, [\hat{A}, [\hat{A}, \hat{B}]]]] \dots$$

The transformations in eq. (21) have this exact form, and this lemma can therefore be used. Although the task of computing this for our annihilation operators might seem daunting, it turns out to be simpler than it seems by using the above mentioned commutation relations. From eq. (7) we have

$$\hat{U}_{BS}(\delta, \phi) = \exp[\delta(\hat{a}_2^\dagger \hat{a}_1 e^{i\phi} - \hat{a}_1^\dagger \hat{a}_2 e^{-i\phi})].$$

We can identify

$$\hat{A} = \delta(\hat{a}_2^\dagger \hat{a}_1 e^{i\phi} - \hat{a}_1^\dagger \hat{a}_2 e^{-i\phi}),$$

$$\hat{B}_1 = \hat{a}_1,$$

$$\hat{B}_2 = \hat{a}_2,$$

for the two different modes.

We start with $\hat{B}_1 = \hat{a}_1$ and compute all the commutations:

$$\begin{aligned} [\hat{A}, \hat{B}_1] &= \delta[\hat{a}_2^\dagger \hat{a}_1 e^{i\phi} - \hat{a}_1^\dagger \hat{a}_2 e^{-i\phi}, \hat{a}_1] = \left\{ [\hat{a}_1, \hat{a}_1] = [\hat{a}_2^\dagger, \hat{a}_1] = 0 \right\} = -\delta[\hat{a}_1^\dagger \hat{a}_2 e^{-i\phi}, \hat{a}_1] = -\delta e^{-i\phi} [\hat{a}_1^\dagger, \hat{a}_1] \hat{a}_2 = \delta e^{-i\phi} \hat{a}_2 \\ [\hat{A}, [\hat{A}, \hat{B}_1]] &= \delta^2 e^{-i\phi} [\hat{a}_2^\dagger \hat{a}_1 e^{i\phi} - \hat{a}_1^\dagger \hat{a}_2 e^{-i\phi}, \hat{a}_2] = \delta^2 e^{-i\phi} e^{i\phi} [\hat{a}_2^\dagger, \hat{a}_2] \hat{a}_1 = -\delta^2 \hat{a}_1 \end{aligned}$$

Observe that we have returned to \hat{a}_1 . All the following commutations will therefore repeat, and we will get

$$\begin{aligned}\hat{b}_1 &= \hat{a}_1 + \delta e^{-i\phi} \hat{a}_2 - \frac{1}{2!} \delta^2 \hat{a}_1 - \frac{1}{3!} \delta^3 e^{-i\phi} \hat{a}_2 + \frac{1}{4!} \delta^4 \hat{a}_1 + \frac{1}{5!} \delta^5 e^{-i\phi} \hat{a}_2 \\ &= \hat{a}_1 \left[1 - \frac{1}{2!} \delta^2 + \frac{1}{4!} \delta^4 - \dots \right] + \hat{a}_2 e^{-i\phi} \left[\delta - \frac{1}{3!} \delta^3 + \frac{1}{5!} \delta^5 - \dots \right] = \hat{a}_1 \cos \delta + \hat{a}_2 e^{-i\phi} \sin \delta.\end{aligned}$$

Similarly for $\hat{B}_2 = \hat{a}_2$:

$$\begin{aligned}[\hat{A}, \hat{B}_2] &= \delta [\hat{a}_2^\dagger \hat{a}_1 e^{i\phi} - \hat{a}_1^\dagger \hat{a}_2 e^{-i\phi}, \hat{a}_2] = \left\{ [\hat{a}_2, \hat{a}_2] = [\hat{a}_1^\dagger, \hat{a}_2] = 0 \right\} = \delta [\hat{a}_2^\dagger \hat{a}_1 e^{i\phi}, \hat{a}_2] = \delta e^{i\phi} [\hat{a}_2^\dagger, \hat{a}_2] \hat{a}_1 = -\delta e^{i\phi} \hat{a}_1 \\ [\hat{A}, [\hat{A}, \hat{B}_2]] &= \delta^2 e^{i\phi} [\hat{a}_2^\dagger \hat{a}_1 e^{i\phi} - \hat{a}_1^\dagger \hat{a}_2 e^{-i\phi}, -\hat{a}_1] = \delta^2 e^{i\phi} e^{-i\phi} [\hat{a}_1^\dagger, \hat{a}_1] \hat{a}_2 = -\delta^2 \hat{a}_2\end{aligned}$$

and this then leads to

$$\begin{aligned}\hat{b}_2 &= \hat{a}_2 - \hat{a}_1 e^{i\phi} \delta - \frac{1}{2!} \hat{a}_2 \delta^2 + \frac{1}{3!} \hat{a}_1 e^{i\phi} \delta^3 + \frac{1}{4!} \hat{a}_2 \delta^4 + \frac{1}{5!} \hat{a}_1 e^{i\phi} \delta^5 + \dots \\ &= \hat{a}_2 \left[1 - \frac{1}{2!} \delta^2 + \frac{1}{4!} \delta^4 - \dots \right] - \hat{a}_1 e^{i\phi} \left[\delta - \frac{1}{3!} \delta^3 + \frac{1}{5!} \delta^5 - \dots \right] = \hat{a}_2 \cos \delta - \hat{a}_1 e^{i\phi} \sin \delta.\end{aligned}$$

References

- [1] Peter W. Shor. “Polynomial-Time Algorithms for Prime Factorization and Discrete Logarithms on a Quantum Computer”. In: *SIAM Journal on Computing* 26.5 (1997), pp. 1484–1509. DOI: [10.1137/S0097539795293172](https://doi.org/10.1137/S0097539795293172).
- [2] Lov K. Grover. “A fast quantum mechanical algorithm for database search”. In: *Proceedings of the Annual ACM Symposium on Theory of Computing Part F129452* (July 1996), pp. 212–219. ISSN: 07378017. DOI: [10.1145/237814.237866](https://doi.org/10.1145/237814.237866);WGROU:STRING:ACM.
- [3] Frank Arute et al. “Quantum supremacy using a programmable superconducting processor”. In: *Nature* 2019 574:7779 574.7779 (Oct. 2019), pp. 505–510. ISSN: 1476-4687. DOI: [10.1038/s41586-019-1666-5](https://doi.org/10.1038/s41586-019-1666-5).
- [4] Richard P. Feynman. “Simulating physics with computers”. In: *International Journal of Theoretical Physics* 21.6-7 (June 1982), pp. 467–488. ISSN: 00207748. DOI: [10.1007/BF02650179](https://doi.org/10.1007/BF02650179)/METRICS.
- [5] Jens Koch et al. “Charge-insensitive qubit design derived from the Cooper pair box”. In: *Physical Review A* 76.4 (Oct. 2007), p. 042319. ISSN: 10502947. DOI: [10.1103/PhysRevA.76.042319](https://doi.org/10.1103/PhysRevA.76.042319). URL: <https://journals.aps.org/pr/abstract/10.1103/PhysRevA.76.042319>.
- [6] Feng Bao et al. “Fluxonium: An Alternative Qubit Platform for High-Fidelity Operations”. In: *Physical Review Letters* 129.1 (June 2022), p. 010502. ISSN: 10797114. DOI: [10.1103/PhysRevLett.129.010502](https://doi.org/10.1103/PhysRevLett.129.010502). URL: <https://journals.aps.org/prl/abstract/10.1103/PhysRevLett.129.010502>.
- [7] P. Krantz et al. “A quantum engineer’s guide to superconducting qubits”. In: *Applied Physics Reviews* 6.2 (June 2019), p. 21318. ISSN: 19319401. DOI: [10.1063/1.5089550](https://doi.org/10.1063/1.5089550)/570326.
- [8] L. Samuel Braunstein and Peter Van Loock. “Quantum information with continuous variables”. In: *Reviews of Modern Physics* 77.2 (June 2005), p. 513. ISSN: 00346861. DOI: [10.1103/RevModPhys.77.513](https://doi.org/10.1103/RevModPhys.77.513).
- [9] Daniel Gottesman, Alexei Kitaev, and John Preskill. “Encoding a qubit in an oscillator”. In: *Physical Review A* 64.1 (June 2001), p. 012310. ISSN: 10502947. DOI: [10.1103/PhysRevA.64.012310](https://doi.org/10.1103/PhysRevA.64.012310). URL: <https://journals.aps.org/pr/abstract/10.1103/PhysRevA.64.012310>.
- [10] Arne L. Grimsmo, Joshua Combes, and Ben Q. Baragiola. “Quantum Computing with Rotation-Symmetric Bosonic Codes”. In: *Physical Review X* 10.1 (Mar. 2020), p. 011058. ISSN: 21603308. DOI: [10.1103/PhysRevX.10.011058](https://doi.org/10.1103/PhysRevX.10.011058).
- [11] Rabsan Galib Ahmed, Adithi Udupa, and Giulia Ferrini. “Multimode rotationally symmetric bosonic codes from group-theoretic construction”. In: ().
- [12] Marios H. Michael et al. “New Class of Quantum Error-Correcting Codes for a Bosonic Mode”. In: *Physical Review X* 6.3 (July 2016), p. 031006. ISSN: 21603308. DOI: [10.1103/PhysRevX.6.031006](https://doi.org/10.1103/PhysRevX.6.031006). URL: <https://journals.aps.org/prx/abstract/10.1103/PhysRevX.6.031006>.
- [13] Steven M. Girvin. “Introduction to Quantum Error Correction and Fault Tolerance”. In: *SciPost Physics Lecture Notes* 70 (Jan. 2023). DOI: [10.21468/SciPostPhysLectNotes.70](https://doi.org/10.21468/SciPostPhysLectNotes.70). URL: <http://arxiv.org/abs/2111.08894><http://dx.doi.org/10.21468/SciPostPhysLectNotes.70>.
- [14] Shruti Puri et al. “Stabilized Cat in a Driven Nonlinear Cavity: A Fault-Tolerant Error Syndrome Detector”. In: *Physical Review X* 9.4 (Oct. 2019), p. 041009. ISSN: 21603308. DOI: [10.1103/PhysRevX.9.041009](https://doi.org/10.1103/PhysRevX.9.041009). URL: <https://journals.aps.org/prx/abstract/10.1103/PhysRevX.9.041009>.
- [15] Michael A. Nielsen and Isaac L. Chuang. *Quantum Computation and Quantum Information*. 10th Anniversary Edition. Cambridge: Cambridge University Press, 2010.

- [16] Howard J. Carmichael. “Statistical Methods in Quantum Optics 1”. In: *Statistical Methods in Quantum Optics 1* (1999). DOI: [10.1007/978-3-662-03875-8](https://doi.org/10.1007/978-3-662-03875-8).
- [17] Klaus Mølmer, Yvan Castin, and Jean Dalibard. “Monte Carlo wave-function method in quantum optics”. In: *JOSA B, Vol. 10, Issue 3, pp. 524-538* 10.3 (Mar. 1993), pp. 524–538. ISSN: 1520-8540. DOI: [10.1364/JOSAB.10.000524](https://doi.org/10.1364/JOSAB.10.000524).
- [18] E. N. Bashmakova, S. B. Korolev, and T. Yu Golubeva. “Bosonic quantum error correction using squeezed Fock states”. In: *Physical Review A* 112.3 (Sept. 2025), p. 032434. ISSN: 24699934. DOI: [10.1103/97yt-nzg2](https://doi.org/10.1103/97yt-nzg2). URL: <https://journals.aps.org/pr/abstract/10.1103/97yt-nzg2>.
- [19] Philip Reinhold. “Controlling Error-Correctable Bosonic Qubits”. In: (2020).
- [20] David S. Schlegel, Fabrizio Minganti, and Vincenzo Savona. “Quantum error correction using squeezed Schrödinger cat states”. In: *Physical Review A* 106.2 (Aug. 2022), p. 022431. ISSN: 24699934. DOI: [10.1103/PhysRevA.106.022431](https://doi.org/10.1103/PhysRevA.106.022431).
- [21] Timo Hillmann et al. “Performance of Teleportation-Based Error-Correction Circuits for Bosonic Codes with Noisy Measurements”. In: *PRX Quantum* 3.2 (May 2022), p. 020334. ISSN: 26913399. DOI: [10.1103/PRXQuantum.3.020334](https://doi.org/10.1103/PRXQuantum.3.020334).
- [22] Bikun Li et al. “Optimality Condition for the Petz Map”. In: *Physical Review Letters* 134.20 (May 2025), p. 200602. ISSN: 10797114. DOI: [10.1103/PhysRevLett.134.200602](https://doi.org/10.1103/PhysRevLett.134.200602).
- [23] Julius Andersson et al. *TRIBE: Two-Mode Rotation-Symmetric Bosonic Code Error Bias*. Version 1.0. Dec. 2025. URL: <https://github.com/cibbe/TRIBE>.
- [24] Lea Lautenbacher et al. “Petz recovery maps for qudit quantum channels”. In: *Physics Letters A* 512 (July 2024), p. 129583. ISSN: 0375-9601. DOI: [10.1016/j.physleta.2024.129583](https://doi.org/10.1016/j.physleta.2024.129583). URL: <http://dx.doi.org/10.1016/j.physleta.2024.129583>.
- [25] J. J. Sakurai and Jim Napolitano. *Modern Quantum Mechanics*. 3rd ed. Cambridge University Press, 2020. ISBN: 9781108473224.

